

# Impacts of Global Warming on Hydrological Cycles in the Asian Monsoon Region

Koji DAIRAKU<sup>\*1</sup>, Seita EMORI<sup>2</sup>, and Toru NOZAWA<sup>3</sup>

<sup>1</sup>*Storm, Flood, and Landslide Research Department, National Research Institute for Earth Science and Disaster Prevention, Tsukuba, Japan*

<sup>2</sup>*Climate Risk Assessment Research Section, Center for Global Environmental Research, National Institute for Environmental Studies, Tsukuba, Japan*

<sup>3</sup>*Atmospheric Physics Section, Atmospheric Environment Division, National Institute for Environmental Studies, Tsukuba, Japan*

(Received 16 May 2007; revised 3 March 2008)

## ABSTRACT

The hydrologic changes and the impact of these changes constitute a fundamental global-warming-related concern. Faced with threats to human life and natural ecosystems, such as droughts, floods, and soil erosion, water resource planners must increasingly make future risk assessments. Though hydrological predictions associated with the global climate change are already being performed, mainly through the use of GCMs, coarse spatial resolutions and uncertain physical processes limit the representation of terrestrial water/energy interactions and the variability in such systems as the Asian monsoon. Despite numerous studies, the regional responses of hydrologic changes resulting from climate change remains inconclusive. In this paper, an attempt at dynamical downscaling of future hydrologic projection under global climate change in Asia is addressed. The authors conducted present and future Asian regional climate simulations which were nested in the results of Atmospheric General Circulation Model (AGCM) experiments. The regional climate model could capture the general simulated features of the AGCM. Also, some regional phenomena such as orographic precipitation, which did not appear in the outcome of the AGCM simulation, were successfully produced. Under global warming, the increase of water vapor associated with the warmed air temperature was projected. It was projected to bring more abundant water vapor to the southern portions of India and the Bay of Bengal, and to enhance precipitation especially over the mountainous regions, the western part of India and the southern edge of the Tibetan Plateau. As a result of the changes in the synoptic flow patterns and precipitation under global warming, the increases of annual mean precipitation and surface runoff were projected in many regions of Asia. However, both the positive and negative changes of seasonal surface runoff were projected in some regions which will increase the flood risk and cause a mismatch between water demand and water availability in the agricultural season.

**Key words:** hydrologic change, dynamical downscaling, regional climate model, Asian monsoon region

**Citation:** Dairaku, K., S. Emori, and T. Nozawa, 2008: Impacts of global warming on hydrological cycles in the Asian monsoon region. *Adv. Atmos. Sci.*, **25**(6), 960–973, doi: 10.1007/s00376-008-0960-1.

---

## 1. Introduction

The hydrologic cycle is vital to human life and natural ecosystems. It has complex interactions within the climate system, and it also has an important role in regulating climate stability and variability. The

industrial transformation and human activities may influence the hydrological cycle globally and regionally. The compelling evidence of the attribution of human activities to the hydrologic change and variability has not yet been provided systematically. Faced with threats to human life and natural ecosystems, such as

---

\*Corresponding author: Koji DAIRAKU, dairaku@bosai.go.jp

droughts, floods, and soil erosion, water resource planners must increasingly make future risk assessments (Schnur, 2002). Historically, stable climatic conditions have been assumed for water resource management, planning, and civil engineering designs. However, global climate changes may lead to changes in rainfall events by an enhancement of atmospheric moisture content (Palmer and Räsänen, 2002). Therefore, the hydrologic changes and the impact of these changes constitute a fundamental global-warming-related concern.

Floods and droughts caused by Asian monsoons affect agriculture, water resources, and the economies of many Asian countries where billions of people live and which are characterized by diverse geography. Dairaku and Emori (2006) suggest that the changes in the Asian summer monsoon resulting from climate change will especially affect the hydrological components such as extreme precipitation. Societies in Monsoon Asia must urgently learn how to adapt to climate changes and cope with the large variability of the Asian monsoons. Is the Asian monsoon system resilient to the anthropogenic transformation of land, water, and air? The importance of the coupled human and environment system in the Asian monsoon region is raised as a key question by the Monsoon Asia Integrated Regional Study (MAIRS; Fu et al., 2006). To control water resources in the face of drought, flood, and soil erosion, which frequently present a serious threat to human life and natural ecosystems, predictions and risk assessments are being required more frequently by policy makers.

Hydrologic predictions that account for global climate changes mainly use GCMs (Coe, 2000; Koster et al., 2000; Vörösmarty et al., 2000; Palmer and Räsänen, 2002; Milly et al., 2002). Despite numerous studies, the regional responses of hydrologic changes (atmosphere-ocean-land interactions, precipitation, and extreme events such as droughts and floods) resulting from climate change remain unclear and have many uncertain factors (e.g., model uncertainties, large amplitude of natural variability and anthropogenic influences such as black carbon, deforestation, and irrigation).

One of the approaches dealing with these uncertain inputs and processes in climate prediction is to use ensemble projections that produce predictions in the form of the probability (Collins, 2007). However, this approach is very expensive computationally and cannot deal with the uncertainty associated with spatial resolutions. Though detailed information for regional areas is frequently required, coarse spatial resolutions (those with grid spacing of approximately 300 km) and uncertain physical processes particularly limit the

representation of terrestrial water/energy interactions and the variability and extremes in such systems as the Asian monsoon. Therefore only a very restricted number of regional-scale estimates are available to planners.

To solve this problem, downscaling methods are employed to produce finer scale information from GCMs with coarse spatial resolution. Two kinds of methods are usually employed. One is statistical downscaling, which estimates local scale variables (e.g., precipitation, temperature, and wind) from GCMs usually based on statistical relationships between synoptic-scale conditions and local-scale variables. Another is dynamical downscaling, which is usually achieved by a high-resolution regional climate model (RCM).

The model is conducted in a limited region and driven by lateral boundary conditions obtained from GCMs (so-called nesting). Therefore, the RCM is strongly controlled by the imposed lateral boundaries that bring large-scale circulations down into the RCM domain. Therefore, it is strongly desired that the boundary conditions are as accurate as possible and the simulated synoptic circulations of RCM should not be greatly different from those of the GCM.

Mesoscale atmospheric systems can be categorized into two groups. The first group is surface inhomogeneities-induced mesoscale systems such as sea and land breezes, mountain valley winds, urban circulations, and forced airflow over rough terrain. The second group is synoptically-induced mesoscale systems such as fronts, squall lines, and hurricanes (Pielke et al., 2002). Because of the higher resolution, the RCM is expected to have the advantage of higher accuracy and the ability to "add value" in small-scale features not well represented by the GCM (Castro et al., 2005).

Surface boundary forcing, such as topography, is the dominant factor for generating small-scale atmospheric variability (Wang et al., 2004), therefore a higher resolution simulation by the RCM is expected to be able to improve the regional circulation pattern and produce realistic intensities and frequencies for mesoscale features, such as orographic precipitation resulting from realistic topography. These mesoscale features can be considered as a boundary value problem.

On the other hand, the synoptically induced mesoscale systems are not necessarily improved by a higher resolution simulation by the RCM. As mentioned above, it is necessary that the boundary conditions are as accurate as possible. And also, the adequate representation of physical processes may be necessary. Therefore, model physics has been an im-

portant issue. One of the strategies in the dynamical downscaling by the RCM is to have a “physics compatibility” with the host GCM. That is, the full physics in the GCM used to provide driving conditions for the RCM is implemented in the RCM. The physics compatibility between the RCM and the host GCM enables the interpretation of the downscaled results to be relatively simple. However, because a physical parameterization such as a cumulus convection scheme can have a significant sensitivity to horizontal resolution, physics schemes developed and tuned for the GCM with coarse horizontal resolution may not be adequate for the nested RCM with the high horizontal resolutions (Giorgi and Mearns, 1999).

In this paper, an attempt of the dynamical downscaling using an RCM having a fully compatible physics schemes with the host GCM is addressed. Also, the influences of anthropogenic activities on the maintenance and variability of regional hydrological cycles in the Asian monsoon region were investigated under global climate change.

## 2. Model and experiments

The model physics in RCMs are a matter of great concern. The differences in the physics parameterizations between an RCM and the host GCM to drive the RCM can often indicate different behaviors because the different physics schemes might cause spurious circulations in the nested interior domain. In addition, similar behaviors obtained from different models can result from different causes (Takayabu et al., 2007). Thereby, the interpretation of the downscaled results can be quite difficult. The physics compatibility between the RCM and the GCM may have the advantage in the interpretation of the results (Giorgi and Mearns, 1999).

We developed a regional climate model based on the strategy to maximize the physics compatibility between the nested RCM and the host GCM as much as possible. A regional climate model was developed, NIES-RAMS (Emori et al., 2001), which is based on a three-dimensional nonhydrostatic compressible dynamic-equations model (RAMS: Regional Atmospheric Modeling System) developed at Colorado State University (Pielke et al., 1992). For dynamical downscaling using an RCM, which has consistency with the GCM schemes, the full physics of the CCSR/NIES AGCM (Numaguti et al., 1997), Arakawa-Schubert cumulus parameterization (Arakawa and Schubert, 1974), large-scale condensation scheme, a radiation scheme based on the two-stream k-distribution method (Nakajima et al., 2000), the Mellor-Yamada level 2.0 turbulence scheme (Mellor and Yamada, 1974, 1982),

and the soil and vegetation model (MATSIRO: Minimal Advanced Treatments of Surface Interaction and RunOff) developed by Takata et al. (2003) are implemented within the RAMS framework.

The present (1981–1990) and future (2041–2050) Asian regional climates were simulated by the NIES-RAMS nested in the CCSR/NIES AGCM experiment results (6 hourly), whose horizontal resolution is T42 spectral truncation (about  $2.8^\circ$  in each grid). The presumed future climate projection is based on the IPCC SRES-A2 scenario. The present climate was also simulated by the RCM driven by the ECMWF objective reanalysis data (ERA15, 6 hourly) whose horizontal resolution is  $2.5^\circ$ . This is comparable with the RCM’s simulation driven by the AGCM experiment to evaluate the RCM’s performance without the influences of the parent model’s bias. In the RCM experiments, the domain is about  $9600 \times 7100 \text{ km}^2$  and represented by  $161 \times 119$  grids with a spatial resolution of 60 km. The nudging timescale of the lateral boundary is 600 s, and the nudging points from the lateral boundary are 10 grids. In the present Asian climate experiment, the observed SST and sea-ice distributions for 1981–1990 (GISST; Rayner et al., 1996) were used. In the future experiment, a seasonally varying “warming pattern”, which is derived from a transient climate change experiment with CCSR/NIES coupled with an ocean-atmosphere climate model, was added to the observed SST.

## 3. Hydrologic projection in Asia with a regional climate model nested in a general circulation model

### 3.1 Present regional climates

Because the RCM is driven by lateral boundary conditions in a limited region, the simulated synoptic circulations in the RCM is strongly controlled by the

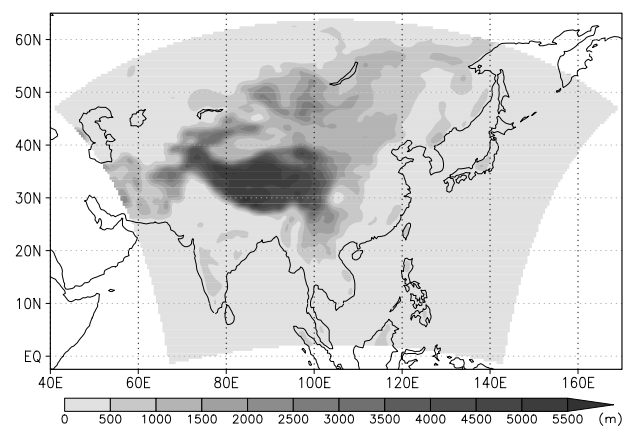
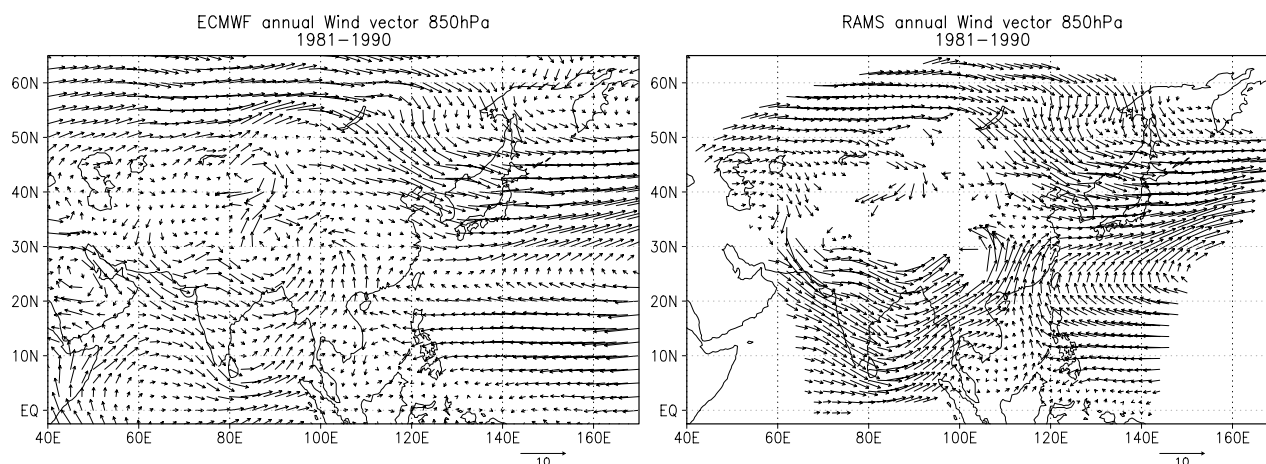


Fig. 1. Simulated region and topography.



**Fig. 2.** Observed and simulated annual mean wind at 850 hPa ( $\text{m s}^{-1}$ ) for 1981–1990. By ERA15 (left), Model (right).

imposed lateral boundaries. The present (1981–1990) climates in the Asian region were simulated by the NIES-RAMS driven by the ERA15 to evaluate the performance. In the future regional hydrological projection by the dynamical downscaling approach, the simulated results can be affected by both the lateral boundary conditions and the implemented model physics. The simulation forced by the objective reanalysis helps to interpret the influence of the model physics on the downscaled projected results.

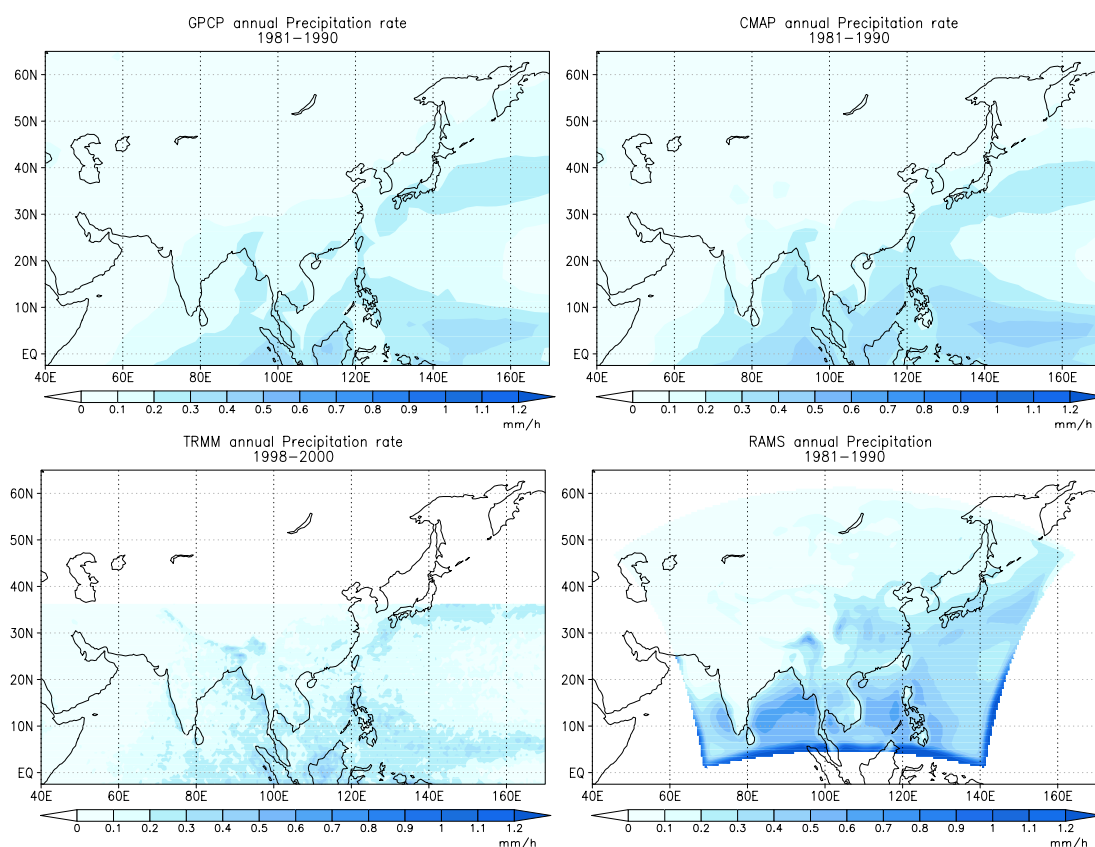
Figure 2 shows the present annual mean wind at 850 hPa (1981–1990) by the ERA15 and the RCM. Basically, the model could capture the general spatial patterns of observed monsoonal flow, flows along the sub tropical high, and westerlies in the mid-high latitude. Though it is reasonable that the simulated wind is relatively stronger than the ERA15 because of the higher resolution of the model, monsoonal flow over East China seems to be exaggerated by the model.

Figure 3 shows the present annual mean precipitation by the Global Precipitation Climatology Project (GPCP; Huffman et al., 1997), the CPC Merged Analysis of Precipitation (CMAP; Xie and Arkin, 1997), the TRMM, and the RCM. The general spatial pattern is relatively well simulated [e.g., annual spatial correlation coefficient between the CMAP (GPCP) and model is 0.85 (0.79)]. The model can capture the surface-induced mesoscale precipitation system (orographic precipitation) on the western side of India and the south-facing slope of the Himalayas, which is observed by the TRMM, though it doesn't appear in the CMAP and GPCP with coarse spatial resolution ( $1^{\circ}$ – $2.5^{\circ}$ ). However, the simulated precipitation over the tropical ocean and over the eastern part of China is apparently overestimated by the model.

The model bias is developed internally by the model dynamics and physical schemes. Compared to

the objective reanalysis (ERA15) used for driving the RCM, the simulated geopotential height is 100–150 m higher than the ERA15, the simulated sea level pressure is systematically lower than observation, in particular over land (4 to 8 hPa), and specific humidity ( $0.002$ – $0.004 \text{ kg kg}^{-1}$ ) is higher over the eastern part of China (not shown). It can be speculated that the RCM has high temperature and low pressure biases particularly over land. The lower pressure over land can cause stronger convergence, increase water vapor, and can produce excessive precipitation over the eastern part of China. Since we took an approach in the dynamical downscaling by the RCM to have a “physics compatibility” with the host GCM, the implemented cumulus convection scheme which is developed and tuned for the GCM with coarse horizontal resolution may not be adequate for the RCM and may overestimate precipitation over the tropical ocean. One of the reasons is that the presumed statistical equilibrium of the cumulus parameterization in a grid may not be properly established with finer grid spacing. The increased latent heat release in the domain can induce the increase of air temperature and thickness.

Suh and Lee (2004) used NCAR RegCM2 for an Asian summer simulation. They reported the positive and negative bias of 2–4 K in temperature over North China and in Mongolia, and excessive precipitation over land, but underestimated precipitation over the southern ocean. It is also reported that RCMs driven by observed boundary conditions have the area averaged temperature biases generally within 2 K and precipitation biases within 50% over the regional scales of  $10^5$  to  $10^6 \text{ km}^2$  (c.f., our simulation region:  $6.9 \times 10^7 \text{ km}^2$ ) (IPCC, 2001). Though it is necessary to improve and tune the model used in this study, the biases in this model are not significantly different from those reported biases.



**Fig. 3.** Observed and simulated annual mean precipitation for GPCP (1981–1990 average) (upper left), CMAP (1981–1990 average) (upper right), TRMM (lower left, 1998–2000 average), and model (1981–1990 average) (lower right).

### 3.2 Dynamical downscaling

In this section, an attempt of the dynamical downscaling and the projected hydrological change using an RCM driven by the GCM are addressed. In this study, the dynamical downscaling is conducted by the RCM using the compatible physics with the host GCM.

The general spatial pattern of synoptic circulations at 850 hPa in the present climate was reasonably simulated by the GCM (Fig. 2 and Fig. 4a). We can find that the monsoon westerly in South Asia simulated by the GCM was overestimated compared to that of the ECMWF Re-Analysis (ERA15). As shown in Figure 4b, the RCM can reasonably capture the general pattern of synoptic circulations at 850 hPa in the present climate, middle-latitude westerlies, and monsoon westerlies, as simulated by the GCM. The spatial pattern of the water vapor flux and precipitation simulated by the RCM is quite similar to that of the GCM (Figs. 4c–f). The RCM improved regional precipitation patterns such as the rain band from the Philippine Islands to the East China Sea and Japan which is associated with Baiu (Mei-yu, Changma) fronts and tropical depressions. An advantage of the dynamical down-

scaling using the RCM can be recognized in surface-forced mesoscale systems (orographic precipitation) in the western side of India and the south-facing slope of the Himalayas, which can not be clearly seen in the GCM with the coarse spatial resolution. Not all precipitation skills improved with the use of the nested RCM. Though the RCM seems to show excellent skills in following the boundary conditions provided by the GCM, it estimated more water flux. Compared to the observations and GCM, the RCM overestimates precipitation in the eastern part of China and in the tropical ocean. Over the eastern part of China, stronger northward wind arises and causes abundant water vapor transport and excessive precipitation. It can be explained by the increased spatial resolution but it might be partly caused by the bias of the RCM, that is, overestimated water vapor convergence induced by the high temperature and low pressure bias over land. The excessive precipitation over the tropical ocean might be attributed to the physics scheme of convection which is not tuned enough for the high horizontal resolution as mentioned in the section 3.1.

Figures 5 show the time-latitude cross section of

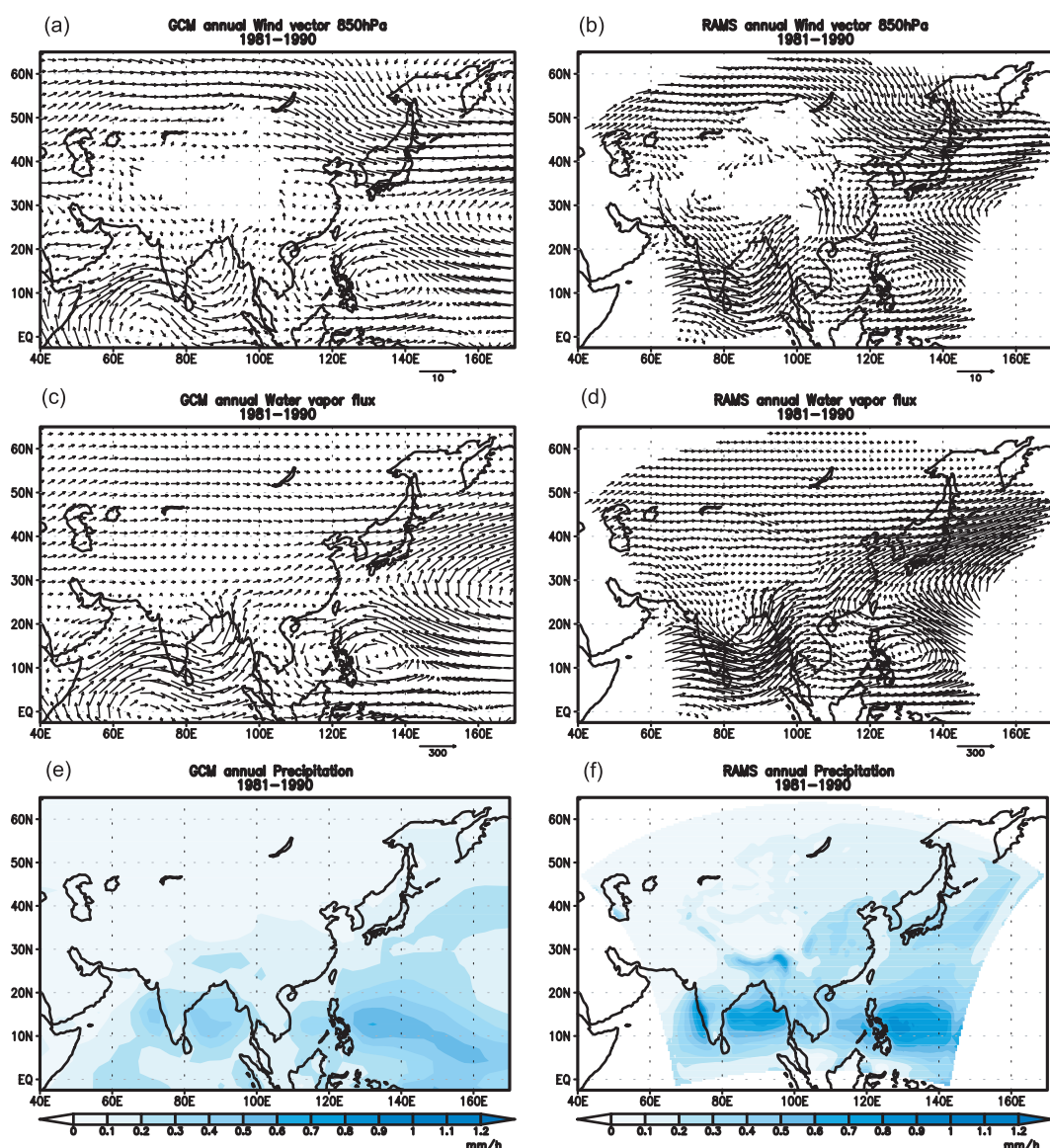


**Fig. 4.** Simulated results averaged for 1981–1990 by the CCSR/NIES AGCM (left panels) and the NIES RAMS (right panels). Also shown are the wind ( $\text{m s}^{-1}$ ) at 850 hPa (upper panels), water vapor flux ( $\text{kg m}^{-1} \text{s}^{-1}$ ) (middle panels), and precipitation ( $\text{mm h}^{-1}$ ) (lower panel).

observed precipitation (GPCP 1dd; Huffman et al., 2001, 1997–2003 average) and simulated precipitation (GCM and RCM, 1981–1990 average). As indicated in the upper panel, a northward migration of relatively strong precipitation is associated with Baiu (Mei-yu, Changma) from May to July. The GCM could not adequately capture the seasonal migration. Though the seasonal migration of precipitation was to some degree augmented by the RCM derived by the GCM as a lateral boundary condition, neither the GCM nor the RCM captures the gradual northward propagation of the monsoon in early summer particularly well.

Though the improvement and tuning of the model

physics schemes is necessary, it can be said that the dynamical downscaling using the developed RCM successfully increased temporal and spatial information in the Asian monsoon region.

### 3.3 Future climate projection in the Asian monsoon region

#### 3.3.1 Annual mean change

About  $1^\circ\text{C}$  increase of the annual mean 2 m air temperature in the tropical region and about a  $3^\circ\text{C}$ – $4^\circ\text{C}$  increase in the mid-to-high latitudinal region are projected from the present climate (1981–1990) to the future (2041–2050) (Fig. 6a). As a result of a stronger

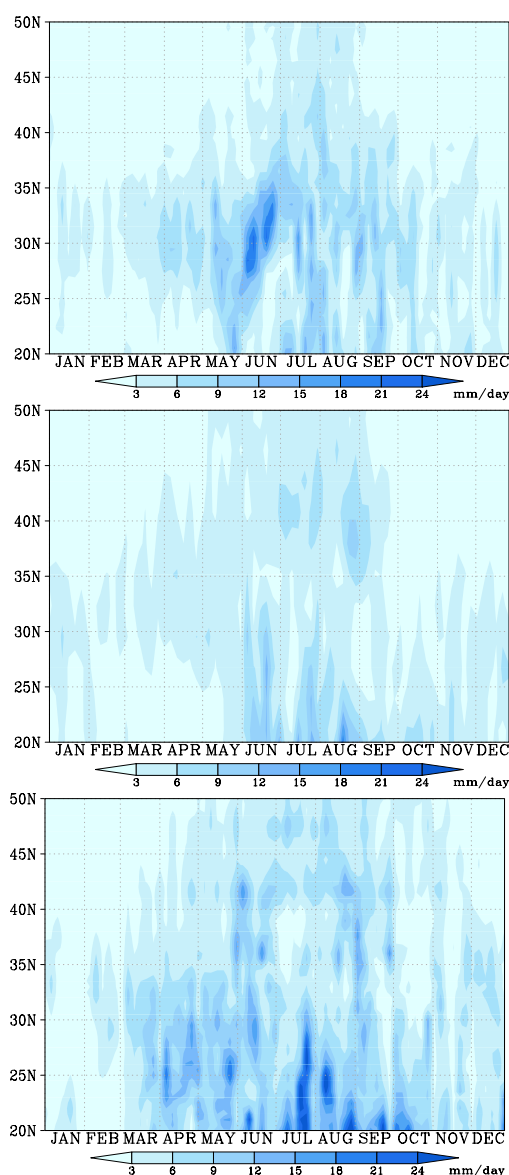


**Fig. 5.** A time-latitude cross section of simulated precipitation at 20°–50°N, 130°E for GPCP-1dd (1997–2003 average) (upper panel), GCM (1981–1990 average) (middle panel), and RCM (1981–1990 average) (lower panel).

temperature increase in the higher latitudes, the meridional gradient of air temperature became weak, and westerlies in the mid-high latitude caused by thermal wind were weakened (Fig. 6c). Responses similar to those of El Niño can be found in projected results by the GCM under global warming. The active convection area over the western Pacific Ocean shifted eastward (not shown). As a result, the Walker circulations were modulated, and the sinking anomaly was formed over the western Pacific. This caused an anti-cyclonic anomaly and a negative anomaly of precipitation over the region in the future climate (Figs. 6b, 6c). An

increase of water vapor and a higher air temperature over the land than over the ocean were projected, enhancing a giant land-sea breeze, the Asian monsoon circulation. Monsoon westerlies in the Arabian Sea, which are associated with the Somali jet, were projected to be stronger and to bring more abundant water vapor to the southern portions of India and the Bay of Bengal (Fig. 6d). It should enhance precipitation especially over the mountainous regions, the western part of India, and the southern edge of the Tibetan Plateau. Increased vapor flux over the region from the Philippine Islands to the East China Sea, which is related with the divergent flow anomaly over the western Pacific Ocean, was also projected. This anomaly increased precipitation in the vicinity of Japan (Fig. 6b). As a result of the aforementioned changes in the synoptic scale-flow patterns and precipitation under global warming, the increase of annual mean surface runoff was projected in many Asian regions (Fig. 6e). It might increase the available water resources and flood risk in the Asian monsoon region.

### 3.3.2 Projected seasonal hydrologic change

In the previous section, the influences of anthropogenic activities on the maintenance and variability of regional hydrological cycles in the Asian monsoon region were indicated. For instance, the increase of annual surface runoff was projected in the Asian monsoon region, however, both the positive and the negative signals of the change of surface runoff were projected in the summer season, which should cause different impacts on each of the regions (Fig. 7).

In this section, the projected impacts of climate change on seasonal hydrologic cycles such as snow, soil moisture, radiation, and evapotranspiration are described. Six regions (South Asia, 5°–25°N, 70°–90°E; Southeast Asia, 7.5°–22°N, 93°–110°E; and Tibet, 28°–38°N, 80°–100°E; East part of China, 24°–37°N, 102°–115°E; Mongolia, 41°–53°N, 87°–120°E; Japan, the region enclosed by the oval in the Fig. 8) were selected to show the changes of seasonal hydrologic cycles. The most of the regions include the mountain zones where the natural and human systems might be easily affected by global environmental change.

#### (1) South Asia (IND)

Dry and rainy seasons associated with Asian monsoon are distinct in South Asia (Fig. 9a). The stronger Monsoon westerlies and associated abundant water vapor are projected to increase precipitation in this region (Fig. 6). The seasonal peak of runoff is almost in accordance with the precipitation. The peak of soil moisture is after a delay of 2 months and it decreases gradually compared to the precipitation and runoff. In the transitional seasons from dry to wet and wet

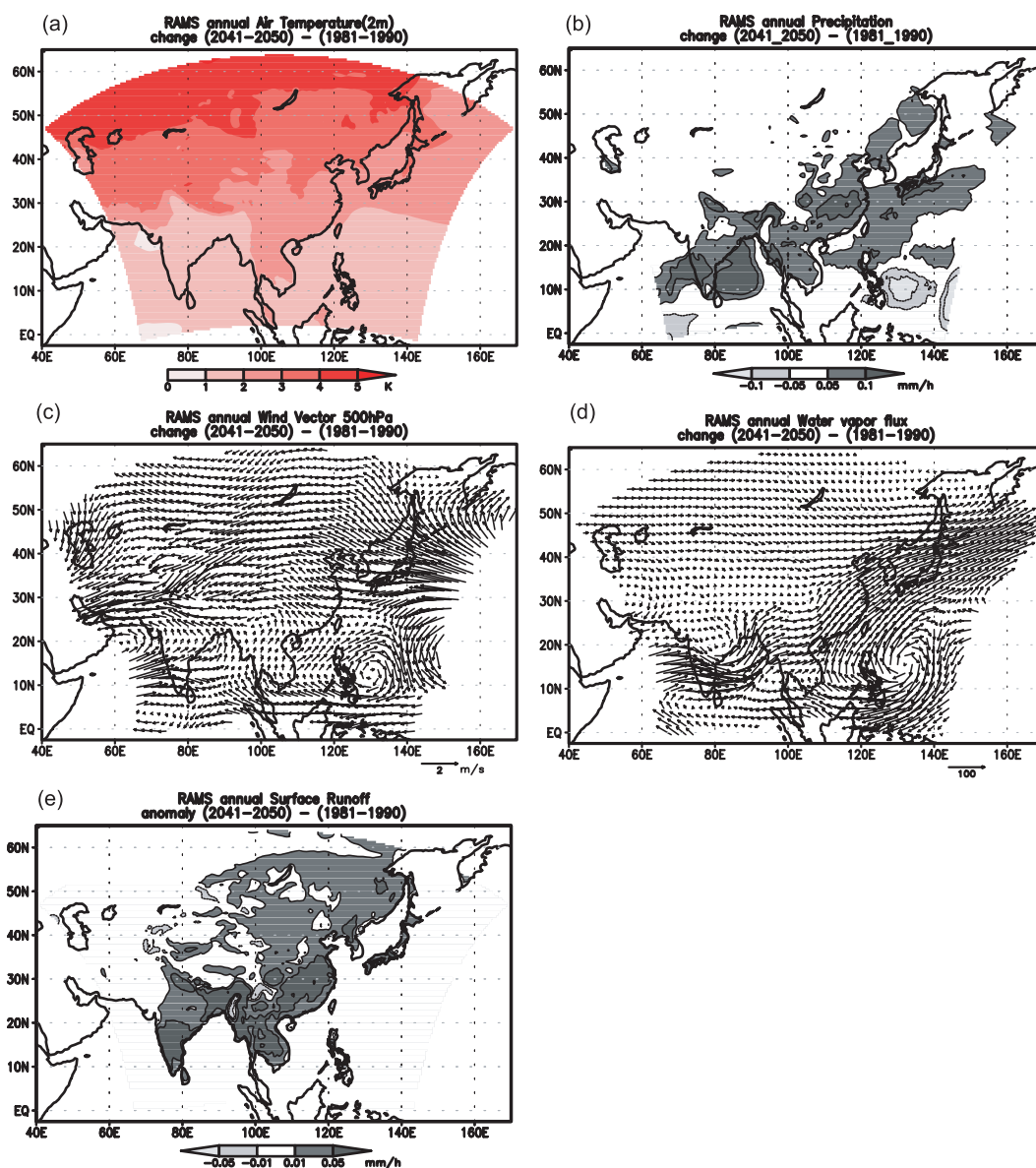


**Fig. 6.** Annually averaged changes of (a) 2 m air temperature (K), (b) precipitation ( $\text{mm h}^{-1}$ ), (c) wind at 500 hPa ( $\text{m s}^{-1}$ ), (d) vertically integrated water vapor flux ( $\text{kg m}^{-1} \text{s}^{-1}$ ), and (e) surface runoff ( $\text{mm h}^{-1}$ ) simulated by the RCM.

to dry, increases of precipitation were projected (Fig. 9b). The increase of large-scale precipitation in the transitional seasons largely contributes to the change. In January and February (dry season), a decrease in convective activities reduce cloud cover and cause an increase of net downward shortwave radiation and a decrease in net downward longwave radiation. As a result, net radiation, sensible heat flux, and latent heat flux increase (Fig. 9c). While the evapotranspiration increases under the climate change, precipitation

doesn't change or is projected to decrease in the dry season. As a result, soil moisture is projected to decrease. Precipitation and runoff are both projected to increase in the transitional seasons. Runoff decreases only in July (Fig. 9d). The increase of convective precipitation in the rainy season augments net downward shortwave radiation by reducing cloud cover. Increase of precipitation, convective activities, and runoff projected in this study would increase flood hazard risks in South Asia.



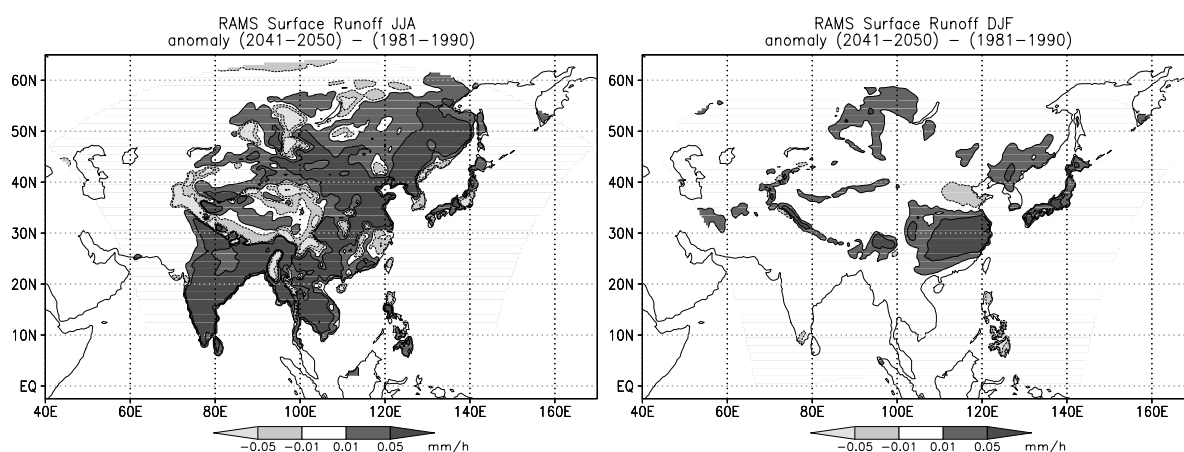


Fig. 7. Seasonal average change of surface runoff of JJA (left panel) and DJF (right panel).

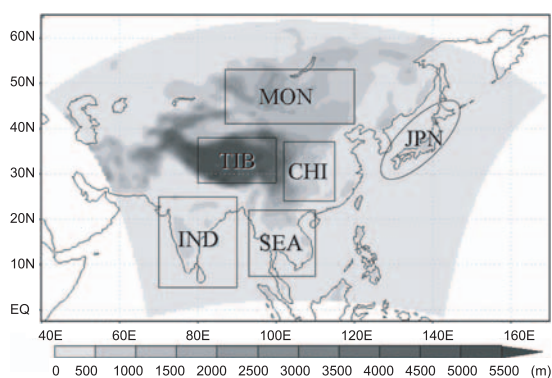


Fig. 8. Selected six regions for seasonal hydrologic analyses and topography.

### (2) Southeast Asia (SEA)

Similar to the South Asia (IND), dry and rainy seasons are distinct in Southeast Asia. In the transitional period from a dry to a wet season, the soil moisture is increased due to increased precipitation and the stream flow increases abruptly as the soil becomes saturated (Fig. 10a). About half of the precipitation is produced by a large-scale condensation scheme, and convective precipitation is predominant in the pre-monsoon season (dry season) (not shown). In the transitional seasons from dry to wet and wet to dry, increases of precipitation, convective precipitation in particular, were projected, while precipitation decreases in the mid-rainy season (June and July) are expected to increase in the region (Fig. 10b). In June and July, the monsoon circulations weaken and precipitation decreases over this region as a result of the intensified high pressure anomaly over the Western Pacific. In the dry season, enhanced convective activities reduce cloud cover and cause an increase of net downward shortwave radiation and a slight decrease of net downward longwave radiation. As a result, net radia-

tion, latent heat flux, and sensible heat flux increase (Fig. 10c). Because the increase of precipitation is relatively small compared to evapotranspiration in the dry season, soil moisture decreases. Although the increases of both precipitation and runoff are projected in the transitional seasons, precipitation, soil moisture, and runoff decrease in the mid-rainy season (June and July) (Fig. 10d). This might lengthen the rainy season and weaken the contrast between dry and wet seasons.

### (3) Tibet (TIB)

In Tibet, a large portion of the precipitation was produced by a large-scale condensation scheme, and in winter, most of it consists of snowfall. Convective precipitation can only be found in summer. Snowmelt has its peak in early summer, and it increases soil moisture and produces more runoff than precipitation (Fig. 11a). As Fig. 11b shows, the increase of precipitation with enhanced convective precipitation was projected particularly in summer. In autumn, rainfall was projected to increase instead of decreasing snowfall resulting from the warming (Fig. 11b). Because of increased incoming energy associated with the enhanced convective activities and the decrease of snowfall, latent heat was projected to increase over the whole year, especially in summer and autumn (Fig. 11c). Because of the decrease of snowfall, an increase of precipitation directly recharges soil moisture in autumn. The decrease of snowfall, an earlier shift of soil moisture and stream-flow peak, and enhanced evapotranspiration will cause a decrease of soil moisture and runoff in summer. These projected changes will reduce the water storage as snow cover in winter, affect the seasonal pattern of stream flow, and possibly influence agricultural activities (Fig. 11d).

### (4) Eastern part of China (CHI)

The seasonal peak of runoff is almost in accordance with the precipitation, though the seasonal change is obscure compared to the aforementioned regions Asia,

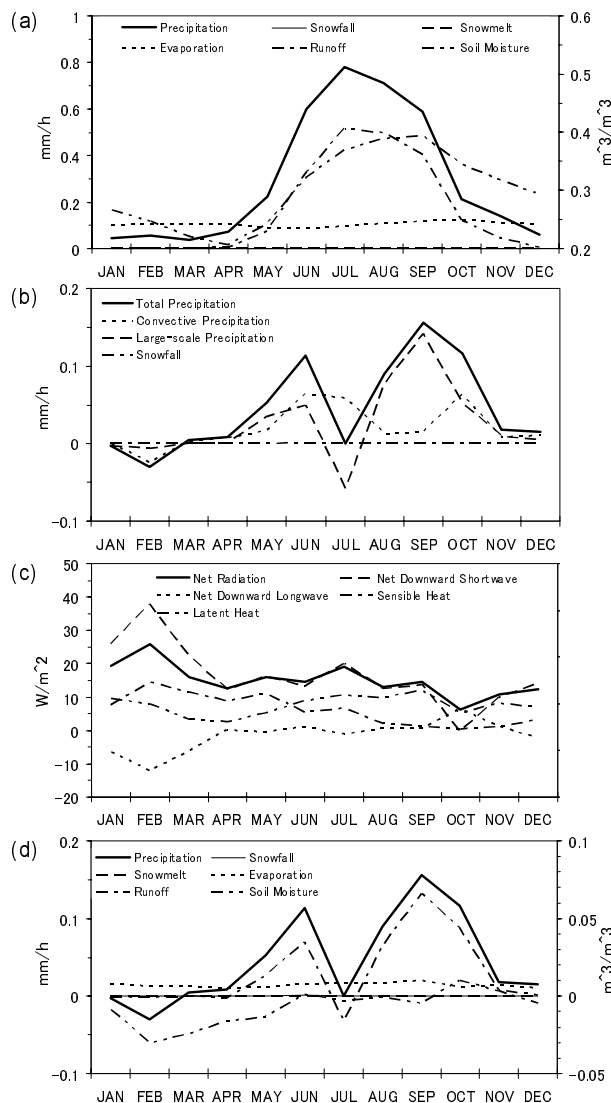


**Fig. 9.** Seasonal hydrologic cycles and projected seasonal changes of hydrologic cycles in South Asia (IND). Simulated seasonal average in 1981–1990 and the changes of 10-year monthly averages, 2041–2050 and 1981–1990, are shown. Also shown are (a) water flux and the changes of (b) precipitation, (c) heat flux, and (d) water flux. Soil moisture ( $m^3 m^{-3}$ ) in (a) and (d) are denoted by the right  $y$ -axis.

Southeast Asia, Tibet). The seasonal change of soil moisture is relatively small and remains in the wet condition (Fig. 12a). A large part of the precipitation was produced by the large-scale precipitation scheme in winter and convective precipitation predominated in summer (not shown). In summer, convective precipitation was projected to increase and made large contributions to the precipitation increase while large-scale precipitation was projected to slightly decrease. In winter, (South snowfall was projected to decrease

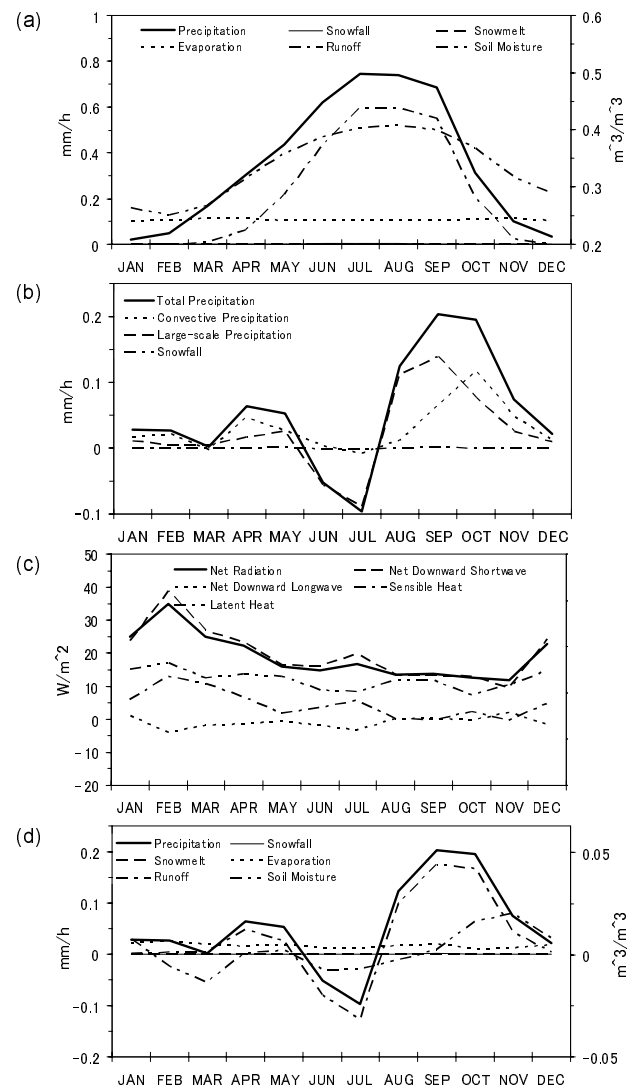


**Fig. 10.** Same as Fig 9 but for Southeast Asia (SEA).

resulting from the warming while rainfall produced by the large-scale precipitation scheme was projected to increase (Fig. 12b). The projected increase of convective activities reduces cloud cover and causes an increase of net downward shortwave radiation and a slight decrease in net downward longwave radiation throughout the year (Fig. 12c). The increased incoming energy and resultant increase of latent heat flux are expected to enhance convective activities and regional water recycling rates. Precipitation and runoff are both projected to increase throughout almost the entire year (Fig. 12d).

As mentioned in section 3.2, overestimated water vapor convergence and excessive precipitation induced by the high temperature and low pressure bias of the model were found over this region. Thereby, the uncertainty of the projected hydrologic changes in this

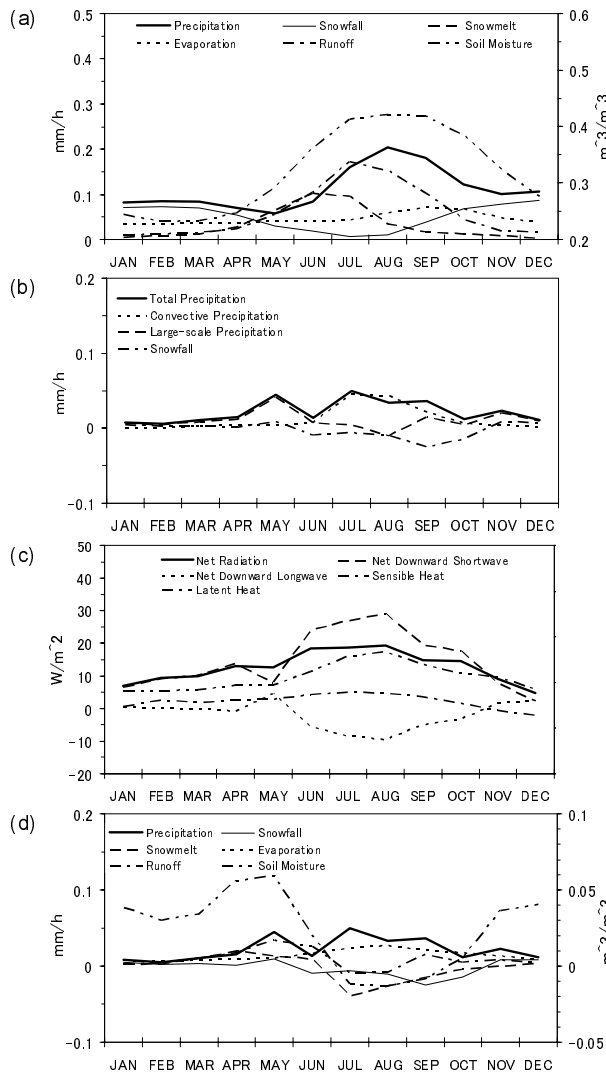


Fig. 11. Same as Fig. 9 but for Tibet (TIB).

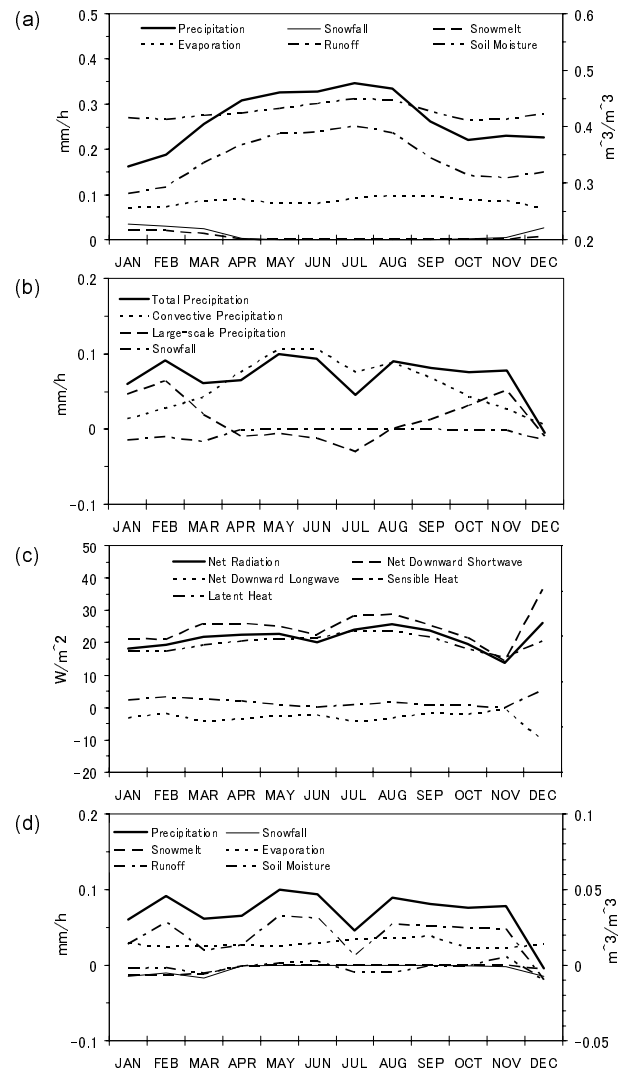


Fig. 12. Same as Fig 9 but for east part of China (CHI).

region might be greater than that in other selected regions. The robustness of the projected changes in this region should be investigated further.

(5) Mongolia (MON)

In Mongolia, a large amount precipitation was produced by a large-scale precipitation scheme, and a large portion of the precipitation falls as snowfall in winter. Convective precipitation increases in summer. Similar to Tibet, snowmelt has its peak in early summer, and it increases soil moisture and runoff (Fig. 13a). The increase in convective precipitation enhanced precipitation particularly in summer while large-scale precipitation slightly decreased. In spring and autumn, snowfall was projected to decrease instead of increase rainfall. Winter snowfall was projected to change little because the increased surface temperature resulting from the warming was projected to be still below 0°C (Fig. 13b). The enhanced convec-

tive activities and the decrease in snowfall increased incoming shortwave radiation, net radiation, and latent heat (Fig. 13c). Because of the decrease of snowfall and an earlier shift of snowmelt resulting from the warming, soil moisture and stream-flow were projected to increase in March and to decrease in following few months (from April to June). The increase of soil moisture and runoff associated with increased convective precipitation was projected in summer (Fig. 13d). The change of the seasonal hydrologic pattern, such as snowmelt and stream flow, may possibly influence agricultural activities.

(6) Japan (JPN)

Similar to the east part of China, soil conditions are relatively wet and the seasonal change is small. The seasonal change of runoff is almost in phase with that of precipitation (Fig. 14a). A large portion of the precipitation was produced by the large-scale precipita-

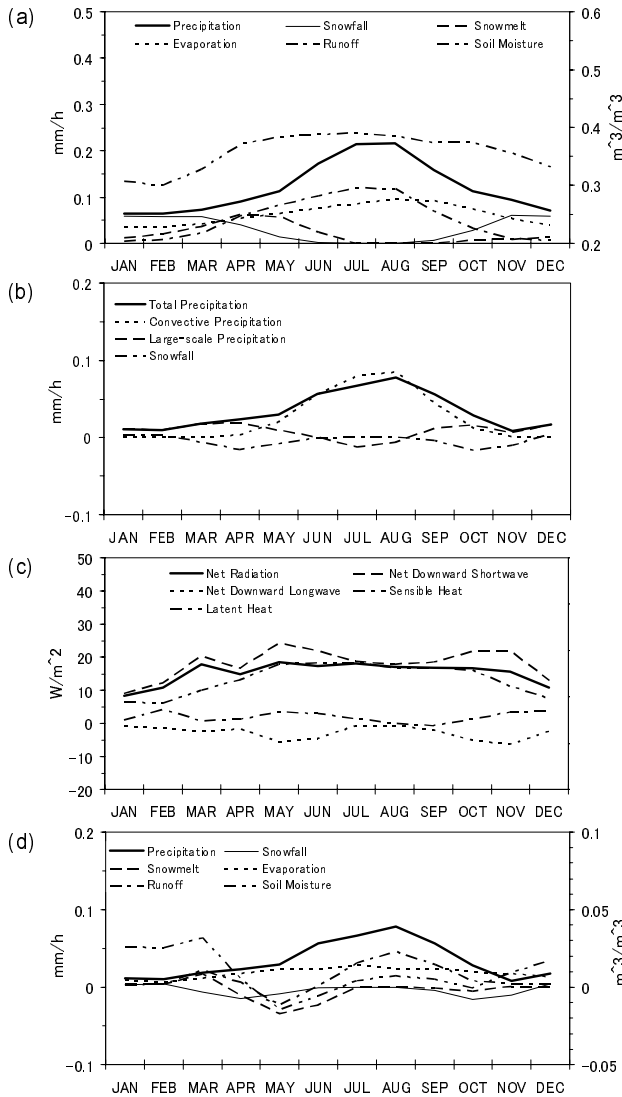


**Fig. 13.** Same as Fig. 9 but for east part of Mongolia (MON).

tion scheme. Convective precipitation was about one third of the precipitation in summer (not shown). Convective precipitation was projected to increase in summer. Large-scale precipitation was projected to increase particularly in winter. Snowfall in spring was projected to decrease while precipitation was projected to increase (Fig. 14b). Because of increased incoming energy associated with the enhanced convective activities and the decrease of snowfall, latent heat flux was projected to increase and a slight increase of sensible heat flux was projected (Fig. 14c). Precipitation was projected to increase for most of the year. The projected change of runoff was in phase with that of precipitation. Because of the increase of evaporation, runoff was projected to decrease slightly in a few

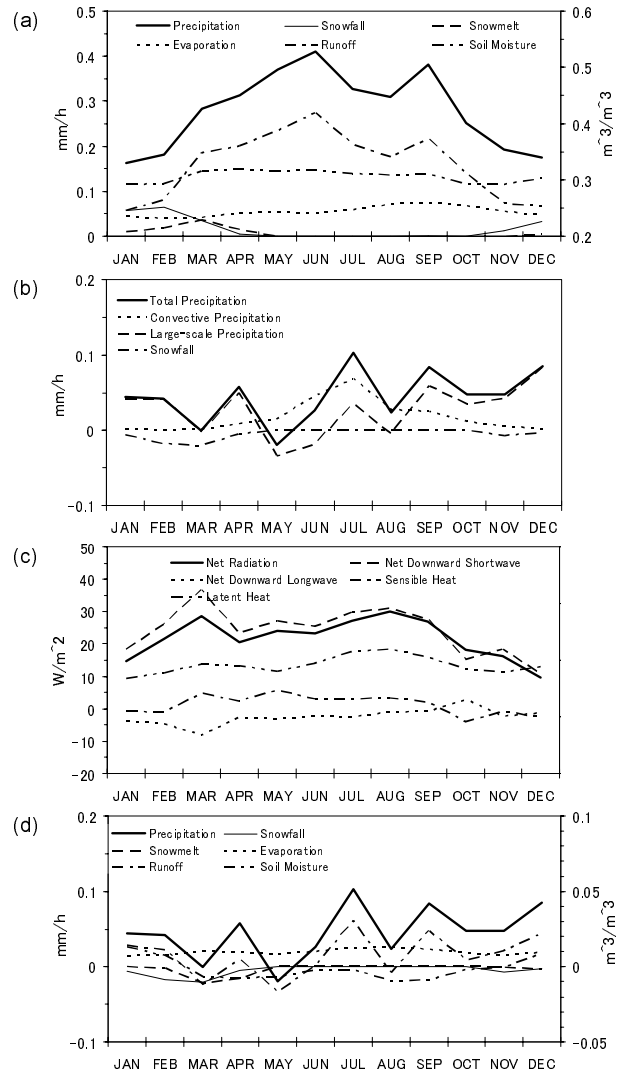


**Fig. 14.** Same as Fig. 9 but for east part of Japan (JPN).

months (March and May) (Fig. 14d).

#### 4. Conclusions

Future hydrologic projection in Asia was conducted by the dynamical downscaling using an RCM, having the physics schemes that are fully compatible with the host GCM. The dynamical downscaling was successful in capturing the synoptic circulation patterns and also in improving some regional phenomena, such as orographic precipitation, which did not appear distinctly in the outcome of the GCM simulation.

Though the physics compatibility between the RCM and the host GCM made the interpretation relatively simple, we found that the RCM had the bias which causes overestimation of precipitation over the eastern part of China and the tropical ocean. It

might be partly attributed to the implemented cumulus convection scheme and large scale condensation scheme which are developed and tuned for the GCM with coarse horizontal resolution. The model physics should be improved and tuned for the RCM with the high horizontal resolutions to reduce the uncertainty of the results.

The influences of anthropogenic activities on the maintenance and variability of regional hydrological cycles in the Asian monsoon region were projected under global climate change. About 1°C increase and a 3°C–4°C increase of the annual mean 2 m air temperature from the present climate (1981–1990) to the future (2041–2050) were projected in the tropical regions and in the mid-to-high latitudinal regions, respectively. Weakened westerlies resulting from the weaker meridional gradient of air temperature in the mid-high latitudes, enhanced Monsoon westerlies and water vapor flux in South Asia, and increased vapor flux over the region from the Philippine Islands to the East China Sea, which is related with the divergent flow anomaly over the western Pacific Ocean, were projected. As the result of the changes in these synoptic flow patterns and the increase of water vapor resulting from the warmed air temperature and enhanced evaporation, the increases of precipitation and surface runoff were projected in many Asian regions. However, both the positive and negative changes of seasonal surface runoff partly attributed to the earlier shift of snowmelt were projected in some regions. This will increase the flood risk and might cause mismatch between water demand and water availability in the agricultural season. An increase in convective precipitation, evaporation, and runoff would enhance the hydrological cycle and increase flood hazard risks in the Asian monsoon region unless water resources are effectively managed.

Because dynamical downscaling by a regional climate model is strongly dependent on the results of parent GCMs, the robustness of the projected results in the present study must be assessed further by using ensemble experiments based on high-resolution GCMs or AGCMs that are coupled to a slab ocean model. Also, the high-resolution global climate model has not yet had enough capability to examine regional-scale feedbacks, especially between atmosphere and terrestrial ecosystems. It is necessary to add spatial resolution (less than 30 km grid spacing), by RCM or in GCM, and biophysical and biogeochemical processes to accurately assess critical synoptic/regional interactions within the Asian monsoon system which is characterized by diverse geography.

Though the investigation of the resilience and vulnerability of the human society in the Asian monsoon region to the global climate change is beyond the

scope of this study, the projected hydrologic changes might have significant influences on social development and human well-being. The social and technological development may have a potential to reduce the social vulnerabilities to natural disasters by employing effective risk management. However, inconsiderate development might worsen the social vulnerabilities. Therefore a further comprehensive study to understand the integrated physical-biogeochemical-human interactions in the Asia monsoon regions is needed.

**Acknowledgements.** This study was conducted as one of the research activities of “Water Resources and Variability in Asia in the 21st Century” of the Research Fund to Promote Science and Technology of Japan’s Ministry of Education, Culture, Sports, Science and Technology (MEXT) supervised by Dr. A. Kitoh of the Meteorological Research Institute of the Japan Meteorological Agency. The work was partially supported by the Global Environment Research Fund of Japan’s Ministry of the Environment (S-5-3). The data used in this study were acquired as part of the Tropical Rainfall Measuring Mission (TRMM). The algorithms were developed by the TRMM Science Team. The data were processed by the TRMM Science Data and Information System (TSDIS) and the TRMM Office.

## REFERENCES

- Arakawa, A., and W. H. Schubert, 1974: Interaction of a cumulus cloud ensemble with the large-scale environment, Part I. *J. Atmos. Sci.*, **31**, 674–701.
- Castro, C. L., R. A. Pielke Sr., and G. Leoncini, 2005: Dynamical downscaling: Assessment of value retained and added using the Regional Atmospheric Modeling System (RAMS). *J. Geophys. Res.*, **110**, doi: 10.1029/2004J.
- Coe, M. T., 2000: Modeling terrestrial hydrological systems at the continental scale: Testing the accuracy of an atmospheric GCM. *J. Climate*, **13**, 686–704.
- Collins, M., 2007: Ensembles and probabilities: A new era in the prediction of climate change. *Philos. Trans. Roy. Soc. London A*, **365**, 1957–1970.
- Dairaku, K., and S. Emori, 2006: Dynamic and thermodynamic influences on intensified daily rainfall during the Asian summer monsoon under doubled atmospheric CO<sub>2</sub> conditions. *Geophys. Res. Lett.*, **33**, L01704, doi: 10.1029/2005GL024754.
- Emori, S., T. Nozawa, A. Numaguti, and I. Uno, 2001: Importance of cumulus parameterization for precipitation simulation over East Asia in June. *J. Meteor. Soc. Japan*, **79**, 939–947.
- Fu, C., F. W. T. Penning de Vries, Ailikun, C. T. A. Chen, L. Lebel, M. Manton, A. Snidvongs, and H. Virji, Eds, 2006: The initial science plan of the Monsoon Asia Integrated Regional Study. MAIRS-IPO,

- IAP-CAS, Beijing, China, 80pp.
- Giorgi, F., and L. O. Mearns, 1999: Introduction to special section: Regional climate modeling revisited. *J. Geophys. Res.*, **104**, 6335–6352 98JD02072.
- Huffman, G. J., and Coauthors, 1997: The Global Precipitation Climatology Project (GPCP) combined precipitation dataset. *Bull. Amer. Meteor. Soc.*, **78**, 5–20.
- Huffman, G. J., R. F. Adler, M. M. Morrissey, D. T. Bolvin, S. Curtis, R. Joyce, B. McGavock, and J. Susskind, 2001: Global precipitation at one-degree daily resolution from multisatellite observations. *J. Hydrometeor.*, **2**, 36–50.
- IPCC, 2001: *Climate Change 2001: The Scientific Basis. Contribution of Working Group I to the Third Assessment Report of the Intergovernmental Panel on Climate Change*. Houghton et al., Eds., Cambridge University Press, Cambridge, United Kingdom and New York, NY, USA, 881pp.
- Koster, R. D., M. J. Suarez, and M. Heiser, 2000: Variance and predictability of precipitation at seasonal-to-interannual timescales. *J. Hydrometeor.*, **1**, 26–46.
- Mellor, G. L., and T. Yamada, 1974: A hierarchy of turbulence closure models for planetary boundary layers. *J. Atmos. Sci.*, **31**, 1791–1806.
- Mellor, G. L., and T. Yamada, 1982: Development of a turbulence closure model for geophysical fluid problems. *Rev. Geophys.*, **20**, 851–875.
- Milly, P. C. D., R. T. Wetherald, K. A. Dunne, and T. L. Delworth, 2002: Increasing risk of great floods in a changing climate. *Nature*, **415**, 514–517.
- Nakajima, T., M. Tsukamoto, Y. Tsushima, A. Numaguti, and T. Kimura, 2000: Modelling of the radiative process in an atmospheric general circulation model. *Appl. Opt.*, **39**, 4869–4878.
- Numaguti, A., M. Takahashi, T. Nakajima, and A. Sumi, 1997: Description of CCSR/NIES Atmospheric General Circulation Model. CGER's Supercomputer Monograph Report. 3, Center for Global Environmental Research, National Institute for Environmental Studies, 1–48.
- Palmer, T. N., and J. Rälsänen, 2002: Quantifying the risk of extreme seasonal precipitation events in a changing climate. *Nature*, **415**, 512–514.
- Pielke, R. A., and Coauthors, 1992: A comprehensive meteorological modeling—RAMS. *Meteor. Atmos. Phys.*, **49**, 69–91.
- Pielke, Sr. R. A., Ed., 2002: *Mesoscale Meteorological Modeling*. 2nd ed., Academic Press, 676pp.
- Rayner, N. A., E. B. Horton, D. E. Parker, C. K. Folland, and R. B. Hackett, 1996: Version 2.2 of the global sea-ice and sea surface temperature data set, 1903–1994. Climate Research Technical (CRTN) No. 74, 43pp. [Available from The Met Office, London Road, Bracknell, UK]
- Schnur, R., 2002: The investment forecast. *Nature*, **415**, 483–484.
- Suh, M. -S., and D.-K. Lee, 2004: Impacts of land use/cover changes on surface climate over east Asia for extreme climate cases using RegCM2. *J. Geophys. Res.*, **109**, doi: 101029/2003J.
- Takata, K., S. Emori, and T. Watanabe, 2003: Development of the minimal advanced treatments of surface interaction and runoff. *Global and Planetary Change*, **38**, 209–222.
- Takayabu, I., H. Kato, K. Nishizawa, Y. N. Takayabu, Y. Sato, H. Sasaki, K. Kurihara, and A. Kitoh, 2007: Future projections in precipitation over Asia simulated by two RCMs nested into MRI-CGCM2.2. *J. Meteor. Soc. Japan*, **85**, 511–519.
- Vörösmarty, C. J., P. Green, J. Salisbury, and R. B. Lammers, 2000: Global Water Resources: Vulnerability from Climate Change and Population Growth. *Science*, **289**, 284–288.
- Wang, Y., L. R. Leung, J. L. McGregor, D.-K. Lee, W.-C. Wang, Y. Ding, and F. Kimura, 2004: Regional Climate Modeling: Progress, Challenges, and Prospects. *J. Meteor. Soc. Japan*, **82**, 1599–1628.
- Xie, P., and P. A. Arkin, 1997: Global Precipitation: A 17-Year Monthly Analysis Based on Gauge Observations, Satellite Estimates, and Numerical Model Outputs. *Bull. Amer. Meteor. Soc.*, **78**, 2539–2558.